Published in final edited form as:
Exp Neurol. 2011 June ; 229(2): 308–323. doi:10.1016/j.expneurol.2011.02.014.

The Generation of Olfactory Epithelial Neurospheres *in vitro* Predicts Engraftment Capacity following Transplantation *in vivo*

Richard C. Krolewski[1,2], **Woochan Jang**[1], and **James E. Schwob**[1]

[1] Department of Anatomy and Cellular Biology Tufts University School of Medicine 136 Harrison Avenue Boston, MA 02111

[2] Program in Cellular, Molecular, and Developmental Biology Sackler School of Graduate Biomedical Sciences Tufts University School of Medicine 136 Harrison Avenue Boston, MA 02111

Abstract

The stem and progenitor cells of the olfactory epithelium maintain the tissue throughout life and effectuate epithelial reconstitution after injury. We have utilized free-floating olfactory neurosphere cultures to study factors influencing proliferation, differentiation, and transplantation potency of sphere-grown cells as a first step toward using them for therapeutic purposes. Olfactory neurospheres form best and expand most when grown from neonatal epithelium, although methyl bromide-injured or normal adult material is weakly spherogenic. The spheres contain the full range of epithelial cell types as marked by cytokeratins, neuron-specific antigens, E-cadherin, Sox2, and Sox9. Globose basal cells are also prominent constituents. Media conditioned by growth of phorbol ester-stimulated, immortalized lamina propria-derived cells (LP_{Imm}) significantly increases the percentage of *Neurog1eGFP* (+) progenitors and immature neurons in spheres. Sphere-forming capacity resides within selected populations; FACS-purified, *Neurog1eGFP* (+) cells were poorly spherogenic, while preparations from *ΔSox2eGFP* transgenic mice that are enriched for Sox2(+) basal cells formed spheres very efficiently. Finally, we compared the potency following transplantation of cells grown in spheres vs. cells derived from adherent cultures. The sphere-derived cells engrafted and produced colonies with multiple cell types that incorporated into and resembled host epithelium; cells from adherent cultures did not. Furthermore, cells from spheres grown in conditioned media from the phorbol ester-activated LP_{Imm} line gave rise to significantly more neurons after transplantation as compared with control. The current findings demonstrate that sphere formation serves as a biomarker for engraftment capacity and multipotency of olfactory progenitors, which are requirements for their eventual translational use.

Keywords

Olfactory epithelium; 3-D; Neurog1; Sox2; conditioned media; lamina propria; phorbol ester; transplantation

Corresponding author: James E. Schwob Department of Anatomy and Cellular Biology Tufts University School of Medicine 136 Harrison Avenue Boston, MA 02111 jim.schwob@tufts.edu.

APPENDICIES

Appendix A: Legend for Supplementary Figures

INTRODUCTION

The olfactory epithelium (OE), the peripheral apparatus for the sense of smell, is renowned for its ability to replace sensory neurons piecemeal during normal life or rapidly and in bulk, along with all the other epithelial cell types, following injury. Regenerative capacity depends upon the life-long retention and activation by injury of neurocompetent stem cells, of which there appear to be multiple kinds. Two types of basal cells – horizontal basal cells (HBCs) and globose basal cells (GBCs) – function as multipotent progenitor and stem cells under a variety of conditions including normal maintenance and regeneration of the OE (Carter, et al., 2004, Chen, et al., 2004, Huard, et al., 1998, Iwai, et al., 2008, Leung, et al., 2007), and are easily harvested by endoscopically-guided biopsy in the living patient. However, the GBC population is functionally heterogeneous and includes different subtypes that can be discriminated on the basis of transcription factor expression; only a subset of GBCs – most likely the ones that express Sox2 and Pax6 but not the proneurogenic factors Mash1 or Neurog1 – exhibit multipotency(Chen, et al., 2004, Guo, et al., 2010).

Despite the apparent redundancy provided by multiple types of multipotent progenitors, very severe injury to the epithelium causes the loss of neurogenic potency, via the elimination of both kinds of basal cells, and results in replacement of olfactory by respiratory or stratified squamous epithelium (Holbrook, 2003, Naessen, 1971, Nakashima, et al., 1984, Schwob, et al., 1994). In humans, stem cell depletion/destruction/dysfunction appears to be responsible for many cases of hyposmia and dysosmia, and, at least in part, for the decline in sensory function as a consequence of “normal” aging, which afflicts at least 25 % of the population over 65 years old at a significant cost to overall health (Murphy, 2008).

Since the stem and progenitor cells of the olfactory epithelium are accessible for nearly risk-free harvest yet also susceptible to damage, several potential translational applications for them are apparent, including the use of autologous olfactory stem and progenitor cells to repair damage elsewhere in the nervous system and, perhaps as a shorter-term goal, replacement of those olfactory stem and progenitor cells lost *in vivo* in order to alleviate the consequent dysfunction. Study of the olfactory neurocompetent stem and progenitor cells is also likely to inform our understanding of the biology of tissue stem cells in general because of the numerous technical advantages of the system.

Of the many steps along the way to using them for repair purposes or understanding the cellular events and signals regulating their behavior, one of the most problematic, in the case of the olfactory stem and progenitor cells, has been the shortcomings of conventional tissue culture models. OE cells in adherent, essentially 2-D cultures no longer look or behave like their *in vivo* counterparts. Nonetheless, cultures of this sort have provided several insights into the regulation of olfactory progenitor cells (e.g., by BMPs and follistatin) and have been used to highlight a rare capacity for generating large colonies *in vitro* (Carter, et al., 2004, DeHamer, et al., 1994, Gordon, et al., 1995, Mumm, et al., 1996, Shou, et al., 2000, Shou, et al., 1999). However, it is highly significant that epithelial cells grown in 2-D are incapable of engrafting properly following intranasal transplantation and do not participate in the repair of the OE, in contrast with multipotent olfactory progenitor cells that are isolated directly from the epithelium and transplanted immediately after harvest (Chen, et al., 2004, Goldstein, et al., 1998, Jang, et al., 2008). Indeed, studies of various stem and progenitor systems (hematopoietic, epidermal, and mammary) have used transplantation as an exacting assay of cellular functional capacity (Krause, et al., 2001, Purton and Scadden, 2007, Shackleton, et al., 2006).

Accordingly, the development and characterization of a culture system that retains the potency of olfactory stem and progenitor cells for reintroduction *in vivo* would have multiple benefits. As a model that retains important similarities to the cells *in situ*, it could be used as a more rapid and more valid means of identifying and characterizing the nature of the signals that regulate progenitor cell behavior. Moreover, the effect of such signals can be assayed with reference to the consequences on engraftment and repair. Likewise, the culture model should be informative as an assay for the differentiative capacity of specific progenitor cell types *in vitro* and *in vivo* after transplantation and engraftment. Ultimately, to be maximally useful, a culture system has to support the expansion of the population of stem and progenitor cells to accumulate sufficient numbers for translational purposes.

We and others have begun to study culture models of the OE that maintain what is increasingly appreciated as a critical aspect of stem and progenitor biology: complex three–dimensional interactions of cultured cells designed to mimic *in vivo* architecture. Of course, data from other neurogenic and epithelial tissues have shown that free-floating spheroids that form from isolated cells (e.g., neurospheres from the subventricular zone and mammospheres from the mammary epithelium) illuminate various characteristics of stem and progenitor cells (Dontu, et al., 2003, Reynolds and Weiss, 1992, Reynolds and Weiss, 1996, Woodward, et al., 2005) and can engraft following transplantation. We have shown that 3-D epithelial-like structures, which we term spheres, form in air-media interface cultures from olfactory progenitor cells harvested following damage to the adult OE (Jang, et al., 2008). The OE-derived spheres recapitulate numerous features of epithelial regeneration *in vivo*, and also preserve differentiative potency, allowing for engraftment and differentiation into multiple cells types following transplantation, in contrast to adherent cultures (Jang, et al., 2008). Although olfactory epithelial spheres from the air-interface cultures will passage, they cannot be used for large-scale expansion or a throughput assessment of which factor(s) support passaging of olfactory stem cells. More recently, free-floating cultures has been adapted to the olfactory system, and recent data suggest that cells present in these olfactory neurospheres (ONS) express markers of various progenitor cells and may have multi-lineage differentiation capacity (Barraud, et al., 2007, Pixley, et al., 1994, Tome, et al., 2009) (Mona Lisa Khan, 2002, personal communication). These studies demonstrated that ONSs can be generated from OE harvested at different developmental time-points, but the work did not explore the features of the spheres with regard to a number of key issues. These include, of course, the ability of the floating sphere-derived cells to engraft following transplantation. Another has to do with the effect on the ONSs of signals that emerge from the lamina propria (LP), a kind of stroma that is deep to the OE and is capable of driving sphere formation in the air-media interface cultures; in other epithelia, such as breast, stromal cells analogous to the LP cells release molecular signals that drive complex tissue-like assembly *in vitro*. In particular, activation of LP-derived cells has the potential to reveal aspects of the functional regulation of olfactory stem and progenitor cells by modeling the signaling from the lamina propria during development or after injury, in a controlled *in vitro* environment. To that end, phorbol 12-myristate 13-acetate (PMA) is a potent activator of PKC and has been shown to stimulate the release of numerous growth factors or activate growth factor receptor pathways for a variety of cell types, including fibroblasts (Amos, et al., 2005, Montero, et al., 2000).

We present here the results of a set of foundational studies designed to investigate the potential usefulness of ONSs as a model for the complexities of assembling/reconstituting the OE and as an assay for the influence on the OE of specific growth factors and of a more complex, but biologically relevant melange of molecules that derives from the cells of the LP. We describe experiments that relate the formation of ONSs to the proliferative status of the epithelium and identify the cells responsible for this proliferation and ONS-forming capacity. We investigate the effects of conditioned media from LP-derived cells on cell fate

within ONSs. We also describe experiments that seek to correlate findings in the ONS system with outcome in a transplantation assay as an especially stringent assay for the biological relevance of the *in vitro* model.

MATERIAL AND METHODS

Animals

B6.129F1 mice obtained from the Jackson Laboratory were used as the source for normal and lesioned cells put in sphere culture and as transplantation hosts. *ΔSox2eGFP* mice are an ES-cell knock-in line and have been described previously (Ellis, et al., 2004). These mice produce GFP in all Sox2-expressing cells of the olfactory epithelium – GBCs, HBCs, and sus cells. *Neurog1eGFP* is a BAC transgenic line generated by the GENSAT project (Gong, et al., 2003). Constitutive GFP-expressing mice (C57BL/6-Tg(CAG-EGFP)1Osb/S) have been utilized previously for transplantation assays and have been described (Chen, et al., 2004, Okabe, et al., 1997). For all cases involving GFP reporter mice, heterozygotes were used exclusively. All animals were housed in a heat- and humidity-controlled, AALAC-accredited vivarium operating under a 12:12-hour light-dark cycle. All protocols for the use of vertebrate animals were approved by the Committee for the Humane Use of Animals at Tufts University School of Medicine, where the animals were housed and the experiments were conducted.

Isolation of cells for Olfactory Neurosphere Cultures (ONS)

Cells isolated from neonatal, normal adult, and methyl bromide–lesioned olfactory epithelia were dissociated according to a standard protocol, with subtle differences as required for dissection of the tissue. Postnatal day (PND) 0-3 mice were anesthetized by intraperitoneal injection of sodium pentobarbital (200 mg/kg), while adult mice were anesthetized by intraperitoneal injection of 0.6 ml/kg of an induction cocktail (43 mg/ml ketamine, 9 mg/ml xylazine, 1.5 mg/ml acepromazine) and then both were perfused with ice-cold Ringers solution. Olfactory turbinate blocks and septum were dissected in Ringers solution. For lesioned adult animals, the mucosa remained on the bone for *en bloc* dissociation. For normal adult animals, the mucosa was detached from the underlying turbinate and septal bones and minced prior to dissociation. Olfactory mucosa was dissociated by incubating in collagenase (1.0mg/ml) and DNAse (0.05mg/ml) for 30 minutes at 37° C with trituration every 10 minutes using a fire polished pipette. After enzymatic dissociation, cells and tissue were centrifuged for 5 minutes at 250 × *g*. The solution was aspirated and the cells and remaining tissue was washed with DMEM + 10% fetal bovine serum (FBS). After centrifugation, excess media was aspirated, cells were resuspended in the appropriate media, syringe-filtered through a 35 μm nylon mesh, and counted by hemocytometer. Cells were plated on ultra low adhesion plates (Corning) at 7.2×10^4 cells/ml in base growth media (DMEM:F12 at 1:3, 2% B27, 20 ng/ml EGF, 20 ng/ml FGF-2, 50 Units/ml penicillin, 50 μg/ml streptomycin, and 1.25 μg/ml amphotericin B) or other media supplemented with EGF and FGF-2 as described. Every third day *in vitro* the cultures were fed by collecting the media and spheres into a conical tube, gently spinning the samples at 250 × *g* for 5 minutes, aspirating half of the old media, and replacing it with new media containing fresh EGF and FGF-2.

ONS size, number, and mass quantitation

At 7 DIV, ONSs were collected into 20 ml plastic sample cups. Immediately prior to measuring with a Beckman Coulter Multisizer 3, a filtered and degassed solution of glycerol and Isoton II (40% glycerol, 60% Isoton II) was added to the samples to a volume of 20 ml. Six runs of 3 seconds each using a 560 μm aperture attached to the Multisizer 3 were used to collect size, number, and mass data for the ONS cultures. 13 ml of the glycerol/Isoton II

solution was added to the cup to replenish the sample volume after every 2 runs. It is important to note that the solution used to suspend the ONS for analysis by the Multisizer is not perfectly isotonic and may result in subtle shrinking of the ONS. The sheath solution was used for all samples and is added immediately prior to size measurements to minimize any effects on ONS measurements. The density of the samples was set at a standard of 1 g/ml for all experiments in order to calculate the mass of ONSs. Size, number, and mass data were exported into Microsoft Excel for further analysis and graphing. The programs InStat and Prism 5 (both from GraphPad) were used for statistical analysis and additional graphing. For the majority of the assays described below, most of the small debris, single cells, and noise were eliminated by analyzing only those particles measured by the Multisizer to be larger than 50 μm in diameter. This cutoff also complements the use of a 35 μm mesh to filter the cell suspension prior to the original plating in culture. For the kinetic assay six parallel ONS cultures of 182,000 cells each were established from the same litter and total mass was measured for each parallel culture as a function of increased time *in vitro*.

ONS Immunocytochemistry

ONSs were immunostained by two different methods – as whole mounts and as frozen sections. For both methods, ONS were fixed in suspension with 10% buffered formalin, 4% paraformaldehyde, Bouins fluid, or 70% ice cold ethanol, depending on the antigen being detected. For whole mount staining, all steps were carried out in 5 ml polypropylene tubes with short 150 × *g* centrifugation steps between all incubations and washes. Primary antibody incubation was carried out at 4° C for 2-3 days. ONSs were washed in PBS 0.05% Tween-20 three times for 1 hour between primary, secondary and tertiary reagents. Bound primary antibodies were visualized by several fluorescently-conjugated secondary antibodies. At the end of the whole mount staining protocol, Hoechst 33258 was added to the final wash (1 μg/ml) to label nuclei. ONSs were cytospun (Shandon) onto slides, and mounted with p-phenylenediamine (PPD) for imaging. For frozen sections, ONSs were cryoprotected with 30% sucrose in PBS overnight. ONS were gently pelleted by centrifugation at 200 × *g* for 3 minutes, the solution was aspirated and the ONSs in residual solution were transferred into OCT compound (Miles Inc., Elkhart, IN). The ONSs were sectioned on a cryostat (Leica), 10 μm sections were collected on to “Plus” slides (Fisher Scientific) and stored at −20° C until staining. For sections of ONSs, all primary antibodies were incubated overnight at 4° C, visualized with fluorescently conjugated secondaries and mounted with PPD as above. EdU was added to ONS cultures 12 hours prior to fixation at a final concentration of 20 μM. EdU detection was carried out as described by the kit's instructions (Invitrogen Cat. No. C10339) prior to immunostaining. Primary antibodies used for detection of antigens in the ONSs are listed in Table 1.

Tissue processing and Immunohistochemistry

Animals were deeply anesthetized by injection of sodium pentobarbital as above and were transcardially flushed with PBS, then perfused with either 4% paraformaldehyde (Fisher Scientific, Suwanee, GA) in 0.05 M sodium phosphate buffer, pH 7.2, or Zamboni's Fixative. The OE was dissected and the tissue block was post-fixed under vacuum for 2 hours. Tissues were then rinsed with PBS, equilibrated through a gradient of sucrose in PBS (15% followed by 30% for 24 hours each), and then frozen in OCT compound (Miles Inc.,Elkhart, IN). The olfactory mucosa was sectioned as described above for ONS.

Standard laboratory protocols were used to detect expression pattern of individual protein in normal OE. For several of the antigens, adequate labeling requires a set of treatments on the sections prior to incubation with the corresponding antibodies. Briefly, frozen sections were rinsed in PBS for 5 minutes to remove the OCT, puddled with 0.01 M citric acid buffer (pH 6.0) and heated to 90°C for 10 minutes in a commercial food steamer (Guo, et al., 2010).

After cooling, sections were rinsed with PBS briefly before incubating with block (10% serum + 5% Non fat dry milk + 4% BSA + 0.1% Triton X-100) for 15 minutes at room temperature. In all cases, the sections were incubated with primary antibodies overnight at 4° C. Bound primary antibodies were visualized by several fluorescently-conjugated secondary antibodies (Invitrogen and Jackson ImmunoResearch). Primary antibodies used for detection of antigens are listed in Table 1. Pixel intensity measurements for GFP staining on sections of Δ*Sox2eGFP* neonates were performed using the brush selection tool in ImageJ. The average pixel intensity over the entire area measured is reported.

LP_{Imm} Cells and Conditioned Media

The LP_{Imm} cell line was derived from the lamina propria of adult mice. The olfactory mucosa was dissected into 1 mm^2 pieces, and the epithelium was dissociated according to standard protocols (Jang, et al., 2008). The remaining tissue (enriched for lamina propria cells) was placed in 2D culture with serum-containing media. Cells that migrated out of the mucosal tissue over a period of days were overlain with a 10^4 infectious particles per ml (final concentration) of MMLV-derived, replication-incompetent pBABE retroviral vector encoding the SV40 long T antigen-NeoR as insert (Addgene, Inc., Cambridge, MA). After growth and selection in neomycin-containing media, early passages of the immortalized cells were frozen as stocks and named LP_{Imm}. Greater than 90% of the cells contain immunodetectable T antigen; all are resistant to concentrations of neomycin that kill all untransduced cells. Further description of the line is deferred to the Results. Conditioned media was generated from LP_{Imm} cells after a 48 hour incubation of DMEM + 10% FBS + 50 Units/ml penicillin, 50 μg/ml streptomycin, starting when the cells were 70-80% confluent. This media is called LP CM. The same procedure was used for the generation of conditioned media from LP_{Imm} cells that were stimulated by incubation in 100 nM phorbol 12-myristate 13-acetate (PMA) in DMSO at the beginning of the 48-hour period. This media is called LP PMA. In both cases, the conditioned media was collected, centrifuged at 500 × *g* to remove debris and then filtered through a 0.45 μm Millex-HV Durapore PVDF syringe filter (Millipore). Conditioned media kept at 4° C was used within 2 weeks. Otherwise it was aliquoted and kept at −20° C until use.

GFP quantitation using FACS

At 7 DIV, spheres were collected into 5ml polypropylene tubes and spun at 150 × g for 5 minutes at 15° C. Excess solution is aspirated and spheres are resuspended in 350 μL 0.25% Trypsin EDTA (Invitrogen). The spheres were incubated at 37° C for 10 minutes. Trypsin inhibitor (10 μL of 5 mg/ml, Worthington) was then added to each sample. Samples were triturated 20 times with a 200 μL pipette, spun again, and aspirated to approximately 200 μL. Propidium iodide was added to a final concentration of 1 μg/ml prior to flow cytometric measurement of GFP+ cells using the MoFlo cell sorter described above. Data were analyzed using FCS version 3 to set gates and determine the percent of GFP(+) and GFP(−) cells for each sample. Values were exported to Microsoft Excel for graphing and analysis purposes. Statistical tests were performed using InStat and Prism 5.

Transplantation

Cells were dissociated from constitutive GFP–expressing neonatal mice and cultured under spherogenic conditions or in laminin-coated culture flasks. After 8 DIV, spheres were dissociated with collagenase and DNAse as above and filtered through a 35 μm mesh prior to infusion into the nasal cavity of a host mouse. An equal number of cells from parallel adherent cultures was trypsinized and transplanted into lesioned littermates of the host animals used for ONS transplantation. The protocol for transplantation into the MeBr-lesioned OE has been described in detail (Chen, et al., 2004). In brief, host F1 B6.129SvImJ mice were exposed to 170 ppm × 8 hours of MeBr gas 18–24 h before transplantation. On

the day of transplantation, the host mice were anesthetized with intraperitoneal (IP) injection of 0.6 ml/kg of an induction cocktail (43mg/ml ketamine, 9mg/ml xylazine, 1.5mg/ml acepromazine). The GFP-expressing donor cells were resuspended in DMEM and infused into one naris of trachetomized hosts via PE10 tubing inserted to a depth of 7 mm (Becton Dickinson). The procedure was terminated after 3 hours, at which point the fluid was aspirated, the tracheotomy was sutured, and the animals were allowed to recover. Transplant recipients were sacrificed 14 days after the procedure. As indicated, host animals were injected with 40 mg/kg of BrdU (5 mg/ml in PBS) eight days after transplantation. Animals were perfused and fixed with 4% paraformaldehyde for histological and immunocytochemical examination.

Sorting olfactory mucosa for purposes of testing spherogenic capacity of defined cell types

Detailed FACS-based protocols for cell isolation have been reported from our lab (Chen, et al., 2004, Jang, et al., 2007, Jang, et al., 2008). Neonatal *ΔSox2-eGFP*animals were euthanized and cells were dissociated as described above. The same was done with *Neurog1-eGFP* mice. Fluorescence-activated cell sorting (FACS) was performed on a MoFlo cell sorter (Cytomation Inc., Fort Collins, CO) running Summit software (Dako). An Innova 90 argon plasma laser (Coherent, Inc., Santa Clara, CA) was used to excite the cells at 488nm and the samples were gated in FL1 to include only the GFP positive cells. Additional gating on forward and side scatter and on exclusion of propidium iodide (PI) at a concentration of 1 μg/ml was used to limit the sort to live cells (Jang, et al., 2007). Cells were collected in DMEM + 10% FBS solution on ice. After collection, cells were spun for 10 minutes at 200 × *g* to pellet the cells. Excess media was removed, and cells were resuspended in base growth media (DMEM:F12 at 1:3, 2% B27, 20 ng/ml FGF-2, 20 ng/ml EGF, 50 Units/ml penicillin, 50 μg/ml streptomycin, and 1.25 μg/ml amphotericin B). After 7 DIV, sphere size, mass, and number were quantified with a Beckman Coulter Multisizer 3.

RESULTS

The work we present here explores the fundamental features of formation, expansion, and composition of spheres derived from mouse OE by varying the sources of the tissue for culture and *in vitro* conditions. In addition, we assess the capacity of cultured ONS to engraft and participate in the regeneration of a host-lesioned mouse OE following transplantation.

Growth Characteristics of Olfactory Neurospheres

Previous published research has demonstrated that the olfactory mucosa of embryonic and neonatal rodents as well as nasal mucosa from adult humans has the capacity to produce free-floating spheres when cultured under the proper conditions (Barraud, et al., 2007, Murrell, et al., 2005, Othman, et al., 2003, Tome, et al., 2009). We have replicated the findings in the neonatal mucosa when proliferation and neurogenesis are robust and expansive and expanded the range of starting materials that can be used to form ONSs to normal adult olfactory mucosa (11-13 wks old) when neurogenesis has slowed to a low level, and to adult mucosa that is recovering after being lesioned by exposure to methyl bromide 2 days earlier, when proliferation of olfactory progenitor cells is approaching a maximum. The number, size, and appearance of the ONS that form vary as a function of the starting material.

When neonatal tissue is harvested and cultured, sphere formation is robust, and the spheres are roughly spherical, usually solid, and range in size from 10-15 cells in the smallest spheres, to hundreds of cells for the largest spheres, which arise as a result of extended time

in vitro. Objects measuring 25-50 μm were mainly nonviable debris or at most a few adherent cells. Accordingly the analysis was limited to particles greater then 50 μm in diameter, which are true ONSs. The larger ONSs often have small subdomains composed of a single cell type that appear to be "budding" from the main body of the ONS (Fig. 1). Rarely, the spheres appear to be hollow or cyst–like and are relatively translucent on brightfield examination. In contrast, the ONSs derived from lesioned adult epithelium are smaller and subdomains are less apparent than in their neonatal counterparts. ONSs derived from the normal OE are extremely rare and small at the 7 DIV timepoint. Most are formed of only a few cells, which are not as cohesive and spherical as ONSs from neonates. Nonetheless, at extended times *in vitro* (>15–20 DIV) a few ONSs derived from normal adult OE can exceed 100 μm in diameter. Quantitative analysis of the sphere-forming capacity of the three tissue types confirms the results of visual inspection (Fig. 1). Accordingly, cells derived from the neonatal olfactory mucosa were used for all subsequent assays because they were consistently the most efficient at producing ONSs.

As first step toward the eventual use of ONS-grown cells for transplantation, we assayed sphere growth as a function of days in vitro (from 3 to 11 DIV) (Fig. 1). Up to 7 DIV, sphere mass increases rapidly, At which point the mass of spheres plateaus and remains static from that time onward, suggesting an inherent restriction on expansion and growth under these circumstances. Although expansive growth can be reactivated for some tissues in culture by dissociation and replating, several attempts at identifying timing or growth factor conditions that might foster ONS expansion by passaging were unsuccessful; these included alternative means of dissociating the spheres and a number of additional factors, including FGF8, LIF, SCF/Steel, Rho Kinase inhibitor Y-27632 (Sato, et al., 2009), and conditioned media from various cell types. In that regard, our experiences with ONSs parallel findings with mammospheres (C. Kuperwasser, Tufts University School of Medicine, personal communication) and early attempts to establish expansive cultures of gut-derived stem and progenitor cells (Sato, et al., 2009).

Cellular Composition of Olfactory Neurospheres

Compositional analysis was performed on intact and on cryosectioned spheres using a standard panel of immunological reagents that are specific for individual cell types in the OE (Table 1). Cells within ONS express the standard cell–type specific markers found in olfactory epithelium, indicating that the spheres recapitulate the differentiation programs of all cell types of the intact tissue (Table 1, Fig. 2). Most ONSs contained numerous neurons as demonstrated by expression of the neural cell adhesion molecule (NCAM) and neuron-specific beta III tubulin (NST), as seen by staining with monoclonal antibody TuJ1. The NCAM and TuJ1(+) cells concentrate within the body of the ONS, rather than on the surface and often elaborate thin neurites extend multiple cell diameters beyond the cells of origin (insets, Fig. 2C). Spheres also contain cells that are labeled by the sus cell/Bowman's duct-gland markers, cytokeratin-18 (CK18) and E-cadherin. Whole mount staining of spheres with these two antibodies demonstrates that many of the "buds"(which resemble the tight associations characteristic of sus cells *in vivo*) identified on brightfield microscopy are composed almost entirely of compacted CK18(+) cells (Fig. 2A, B). CK18(+) cells are less frequent outside of the "budding" subdomains, but individual CK18(+) cells are found on occasion elsewhere in the spheres. At least some of the CK18(+) cells are also marked by expression of Sox9, a transcription factor expressed in Bowman's duct and gland structures of the OE. Much less frequent are cells that stain with the HBC marker, CK14. Some CK14(+) cells resemble closely the HBCs found *in vivo* (Fig. 2A, inset). The CK14(+) and the CK18(+) cells are mitotically quiescent, for the most part, and did not incorporate the thymidine analogue EdU (Fig. 2). Cells derived from the mesenchyme of the lamina propria and labeled by expression of Thy1.2, a marker of fibroblasts, or PECAM, a marker of

endothelial cells, are infrequent within the spheres (Supplementary Fig. 1, and data not shown, respectively).

Finally, the spheres contain a number of cells that have the molecular profile of GBCs, which are the primary proliferative cell type in the intact OE and are defined as basal cells that do not express CK14 or CK18, but express a variety of transcription factors including Mash1, Neurog1, and Sox2. For purposes of the *in vitro* analysis here, GBCs are defined by a combination of the following criteria: staining for markers of proliferation (Ki67), ability to incorporate thymidine analogs, expression of Sox2 protein, and a lack of CK14 and CK18 expression. A number of the cells in the ONS are proliferating and are labeled by the incorporation of EdU or the expression of Ki67 (Fig. 2). Some of these Ki67(+) cells are also Sox2(+). Direct evidence for the existence of GBC-like cells in ONS comes from the direct comparison of Sox2, CK14 and CK18 expression, which demonstrates that CK14(−)/CK18(−) /Sox2(+) cells are present in the ONSs (Fig. 2E).

Another approach to the identification of GBCs uses transgenic GFP-expressing mouse lines as highly sensitive reporters for transcription factors that are expressed by GBCs, including the SRY-family transcription factor Sox2 (*ΔSox2eGFP*) and for the bHLH transcription factor Neurog1 (*Neurog1GFP*), in order to avoid the problems of relatively low abundance of transcription factor antigens (Fig. 2). The use of these two lines of transgenic mice allows an opportunity to dissect which types of GBCs are found within the spheres, since some of the Sox2(+) GBCs of the OE are multipotent while the Neurog1(+) GBCs seem to be generating neurons directly. Cells isolated from *ΔSox2eGFP* mice and cultured as ONSs contained numerous GFP(+) cells. Staining of spheres with HBC and sus cell markers (CK14 and CK18, respectively), demonstrate that the majority of *Sox2eGFP*(+) cells do not show evidence of HBC or sus cell differentiation. By analogy to *in vivo* patterns of expression, the presence of GFP(+)/CK14(−)/CK18(−) cells that are proliferating and labeled by incorporation of EdU indicates that the spheres contain Sox2(+) GBCs.

Cells isolated from *Neurog1eGFP* mice and cultured as ONS also contained GFP(+) cells. By analogy to the cell types that express *Neurog1eGFP in vivo*, the GFP(+) cells in ONS correspond to a more downstream GBC – namely the immediate neuronal precursor (GBC_{INP}) – as opposed to the GBCs that function as multipotent progenitors or transit-amplifying cells (Fig. 2). Some of the GFP(+) cells also express markers of immature neurons (PGP9.5 and TuJ1), which is also seen *in vivo* and reflects GFP perdurance into the progeny of GBC_{INP} cells.

The expression of GFP in the two lines was also analyzed *in vivo* in neonatal animals in order to validate further their use as markers in spheres. The pattern of GFP labeling in the OE of neonatal *ΔSox2eGFP* animals matches the results from adult OE (Supplementary Fig. 2). Our lab has previously reported that sustentacular cells produce a high level of Sox2 protein, while HBCs and GBCs produce a lower level of Sox2 (Guo, et al., 2010). The levels of GFP in *ΔSox2eGFP* animals follow suit. In contrast with the adult setting, some GFP carries over into the neuronal population. In the epithelium of *Neurog1GFP* mice, GFP marks the vast majority of GBCs that are stained by anti-Neurog1 (approximately 75-85%), indicating that expression of the transgene begins at the same time as the endogenous locus (Supplementary Fig. 3). The GFP(+) basal cells are proliferative as seen by incorporation of BrdU and are distinct from horizontal basal cells as seen by exclusion from CK14(+) staining. However, GFP also remains detectable in downstream NCAM(+) immature neurons that do not label with anti-Neurog1 as a likely consequence of the longer half life of GFP (Supplementary Fig. 3). Nonetheless, the pattern of GFP labeling in the epithelium of the two transgenic lines *in vivo*, particularly with respect to the degree of GFP perdurance

into neurons, is consistent with the interpretation that the Sox2(+) GBCs appear to be upstream of the Neurog1(+) ones in the neonatal epithelium, as well.

Defining sphere-forming capacity of specific types

That the ONSs include all of the various olfactory cell types, including a large fraction that are GBCs, raises the issue of which cell type(s) contribute to and are responsible for the assembly and growth of ONSs. In particular, are the GBCs that express the transcription factor gene *Sox2*, which likely marks the multipotent GBCs, more capable of generating spheres than the GBCs that express *Neurog1*, which marks proliferative GBCs that most likely generate post-mitotic neurons directly? We have used the two mouse lines, *ΔSox2eGFP* and *Neurog1eGFP*, respectively, to explore this question by isolating specific populations by FACS, which are then assayed for their ability to form ONSs in isolation from other cell types.

With regard to the *Neurog1eGFP*(+) line, FACS based on GFP expression was used to isolate two populations: first, GFP(+) GBCs and downstream immature neurons (34% of total PI(−) cells), and second, the GFP(−) population which will be a complex and heterogeneous mixture of other GBCs, HBCs, and additional differentiated cell types of the olfactory mucosa (62% of total) (Fig. 3). Equal numbers of GFP(+) and GFP(−) cells were placed on ultra low adhesion plates and cultured for 7 DIV before analyzing sphere formation. GFP(−) cells formed spheres very well, while GFP(+) cells did so poorly, with the mass of the GFP(−)-derived cultures being more than four times the mass of the ones formed by the GFP(+) isolated cells. These data suggest that Neurog1(+) cells are not able to produce spheres on their own and are unlikely to be solely responsible for the formation and proliferation of ONS seen in unsorted cultures. Control cultures of both GFP(+) and GFP(−) cells plated on laminin-coated standard tissue culture slides demonstrated that cells from both fractions will grow in adherent cultures, indicating that differential viability is not the reason for the difference in ONS-forming capacity (Supplementary Fig. 4). It is important to note that *Neurog1eGFP*(+) cells can integrate into ONS and participate in their growth, as seen in sphere cultures from unsorted *Neurog1eGFP* neonates, just not on their own.

In contrast, the GFP(+) fractions from *ΔSox2eGFP*(+) mice encompass a wider variety of cell types and allows for the separation of specific groups of these cells sorted on the strength of GFP signal that can each be tested for spherogenicity (Fig. 3). Based on the levels of *in vivo* expression of Sox2 protein and of GFP in the *ΔSox2eGFP* mice, three distinct populations are expected to be GFP(+): sustentacular cells, HBCs, and a heterogeneous population of GBCs. On tissue sections, the sustentacular cells are about twice as bright as the basal cells by densitometric image analysis and are thus concentrated among the brightest cells when GFP intensity is assayed by FACS, i.e., the GFP(high) population (Fig. 3). In contrast, the less bright GFP(+) cells, i.e., the GFP (low) population in the FACS profile (Fig. 3), will include HBCs, GBCs, and a few downstream immature neurons that retain GFP at a low and declining level. The level of GFP-labeling in FACS samples was directly determined for the population of HBCs, as they are a likely component and exemplar of the GFP(low) population that can be analyzed separately by combining the sort for GFP-expression level with one for anti-CD54 (also known as ICAM), which is known to surface-label HBCs(Carter, et al., 2004,Guo, et al., 2010). Indeed, all of the CD54(+) cells, i.e., all of the marker-confirmed HBCs, are found within the GFP(low) population, and, conversely, CD54 staining does not shift cells in the GFP(high) population (Supplementary Fig. 5). Post hoc analysis of cytospun cells from each of the three populations of the FACS profile is confirmatory: more than 75% of cells in the GFP(high) population are also CK18(+) in contrast to less than 4% of cells in the GFP(low) population, both of which groups would be sus cells, given the GFP labeling. Likewise, less than 2% of cells in the GFP(low) population are CK18(+), which may correspond to either Bowman's

duct and gland cells, or sus cells that have leaked GFP as a consequence of the FACS protocol. In contrast, the CK14(+) HBCs are largely limited to the GFP(low) population where they constitute 12% vs. the GFP(high) population where they are less than 1% of toral. The GFP(no) population from these animals is expected to contain mature neurons, Bowman's duct and gland cells, and potentially any GBCs that are upstream of and not marked by the expression of Sox2, and any cells released from the lamina propria during dissociation.

Accordingly, *ΔSox2eGFP* neonatal mucosa was dissociated and FACS sorted into a sus cell-enriched, GFP(high) fraction, a basal cell-enriched, GFP(low) fraction, and a neuron/duct/gland/lamina propria-enriched GFP(no) population (Fig. 3). The GFP(high) fraction produces few ONSs (average mass = 2.5×10^{-6} g), while the GFP(low) and the GFP(no) fractions make spheres robustly and to an extent nearly an order of magnitude greater (average mass = 1.8×10^{-5} g and 1.75×10^{-5} g, respectively) than the GFP(high) population. As with the *Neurog1eGFP*-sorted fractions, each *ΔSox2eGFP*-sorted population was cultured on laminin–coated glass slides as an additional control for viability. All three populations contained viable cells that attached and survived in adherent cultures on laminin-coated slides (Supplementary Fig. 4).

Transplantation of Olfactory Neurospheres

The foregoing results indicate that ONSs contain GBCs that are likely to be multipotent and that the capacity for forming ONSs resides, at least in part, with progenitors that are known to be multipotent *in vivo*. Thus, free-floating ONSs satisfy one of the criteria – retention of potentially multipotent progenitor cells – expected of cultures that retain the broad potency needed for transplantation and successful engraftment, in the same way that the complex 3-dimensional structures that form from dissociated cells cultured on inserts maintain that potency (Jang, et al., 2008).

Accordingly, ONSs were dissociated and used for transplantation after an eight–day culture period. The attempted transplantation and engraftment of cells from adherent cultures grown in parallel, served as the control. ONS-derived cells, generated from mice that express GFP constitutively, engrafted following transplantation into 1-day post-methyl bromide host mice and gave rise to colonies that were well incorporated into the regenerating epithelium. For example, at 14 days after transplantation, most of the sphere-derived colonies are in the same focal plane as the adjacent host OE, in keeping with what well-integrated colonies look like when they form with other paradigms (including transplants of acutely isolated sorted or unsorted cells or clones labeled by retroviral transduction of progenitors in the lesioned OE(Chen, et al., 2004, Goldstein, et al., 1998, Huard, et al., 1998, Jang, et al., 2008)). Colonies of this type are classified as “properly incorporated” (Fig. 4). Less often, the transplanted, ONS-derived cells formed a mass attached to the top of the host epithelium that sprawled across its surface. Transplantation of ONS-derived cells into three hosts produced 75 colonies, 55 of which were properly incorporated into the olfactory epithelium, 12 of which appeared to have formed on top of the epithelium, and 8 of which could not be classified on the basis of their appearance in the whole mounts.

In contrast, transplanted cells derived from adherent cultures typically formed “non-incorporated”, excrescent colonies. (Fig. 4). The colonies described as “not incorporated” had irregular and ill-defined borders and were plastered across the surface of the epithelium at a distinctly more superficial focal plane. Often, adherent cell-derived colonies formed within synechiae that bridged opposing regions of olfactory mucosa. Transplantation of adherent culture-derived cells into 3 hosts resulted in 27 colonies, 1 of which was properly incorporated into the olfactory epithelium, 20 of which had not engrafted properly, and 6 of which could not be classified on the basis of their appearance on whole mount. Chi-square

analysis of these data indicate that the distribution of the ONS-derived and adherent cell-derived colonies have significantly different morphologies (Yates Chi-square = 36.999, Yates p–value = 1×10^{-8}).

Selected colonies from both transplantation paradigms were cryosectioned for purposes of more detailed analysis of differentiative potency. ONS-derived colonies that had integrated into the epithelium ("properly incorporated"), indeed resembled the colonies that form when donor cells are transplanted from donor to host immediately after harvesting without an intervening culture period (Chen, et al., 2004). Properly incorporated colonies were composed of all of the typical olfactory cells found in the adjacent host epithelium (for example, the apical nucleus and cytoplasmic foot process characteristic of sus cells, or the apical dendrite of olfactory sensory neurons) and displayed an antigenic profile that confirms the morphological characterization: donor-derived GFP(+) cells that also are PGP9.5(+) and hence neurons vs. GFP(+) apically situated cells that are PGP9.5(−) (Fig. 5). With the exception of GFP expression, the engrafted cells are indistinguishable morphologically and antigenically from endogenous host olfactory epithelial cells.

In stark contrast with the colonies derived from ONS–derived cells, the donor-derived cells in the "not incorporated", excrescent colonies, i.e., the predominant type of colony that forms after transplantation of cells grown in adherent culture, consist of cells with a mesenchymal, i.e., spindle cell or fibroblastic, morphology. Rarely, if ever do the cells in these excrescent colonies resemble the constituent cells types found in the surrounding host epithelium (Fig. 5).

Effects of Conditioned Media from Lamina Propria–Derived Cells on ONS

The foregoing demonstrates that the ONSs retain the capacity to engraft and the potency to participate fully in the reconstitution of the cells types of the olfactory epithelium, even though the cultures, as currently constituted, do not expand on passaging. The experience of other tissues in complex culture suggest that cues external to epithelial cells are critical to their capacity to be passaged and will also alter the composition of the cultures that form, the exception being CNS-derived neurospheres, which are remarkable for their capacity to expand in very simple media. That the ONSs contain several subtypes of GBCs, as well as other stem and progenitor cell candidates (HBCs and Bowman's duct/gland cells) and more differentiated cells, suggests that the cells needed to accomplish extensive proliferation and self–renewal are present, but are missing the necessary signals or cues to do so. In contrast to the intact tissue, mesenchymal/stromal cells are not a prominent component of the spheres (see above and Supplementary Fig. 1), and any modulation of epithelial cell differentiation by them is likely to be muted or missing in ONS cultures. Certainly data from other analogous systems suggest that regulatory signals from stromal components are critical to the development of the tissue.

Accordingly, we developed a line of lamina propria cells (LP_{Imm}) that had been immortalized by retroviral transduction with the SV40 large T antigen (see Material and Methods) as a source of potentially relevant signals that may influence cell growth and differentiation in ONS (Supplementary Fig. 6). The LP_{Imm} cell line is not clonal, but given the complex cellular composition of the lamina propria, clonality may not be desirable. The cells express high levels of vimentin and do not express detectable levels of cytokeratins, suggesting that they are mesenchymal in nature, and most likely fibroblastic given their migratory behavior, as are the cells that stimulate growth in cultures of mammospheres and other tissues. The LP_{Imm} cells have proven effective at stimulating sphere growth in an air–liquid interface model of olfactory epitheliopoiesis (Woochan Jang and James E. Schwob, unpublished data). In addition to standard conditioned media (CM) from LP_{Imm} cells, a parallel culture of these cells were treated with phorbol ester (PMA), which is known to

stimulate the release of multiple growth factors from a variety of cell types(Amos, et al., 2005, Montero, et al., 2000). Admittedly, the use of the LP_{Imm} cell line represents only a first step toward understanding the reciprocal interactions between olfactory stroma and epithelium, but a useful one, nonetheless.

The effects of LP_{Imm}-conditioned media (LP CM) and conditioned media from PMA–treated LP_{Imm} cells (LP PMA) on the growth and composition of ONSs formed from cells of neonatal *Neurog1eGFP* mice was compared with two control media (DMEM with10% FBS; DMEM with 10% FBS and 100 nM PMA). Direct observation by fluorescence microscopy suggested that cultures treated with LP PMA contained more GFP(+) cells, i.e., the GBCs that express Neurog1 and the neurons that come from them. FACS was used to quantify the percent of GFP(+) cells in each condition at 7 DIV and plotted relative to control (Fig. 5). The data indicate that spheres grown in LP PMA contained 2.5-times more GFP(+) cells as compared with the other conditions, a statistically significant difference as a function of condition, including the comparison between LP PMA vs. LP CM media and vs. the control media (Fig. 6). These data suggest that PMA activates the LP cells to release a factor or factors that increase(s) the percentage of GFP(+) cells, and this effect cannot be attributed to PMA acting on the ONS directly. The increase in GFP(+) cells in the LP PMA condition may be due to either increased neurogenesis, increased survival of Neurog1(+) GBC and their GFP(+) progeny, or a combination of both.

ONS culture conditions and the outcome of transplantation

As described above, culturing spheres in LP PMA media altered the composition of the spheres that formed – boosting the percentage of GFP(+) cells in ONSs derived from neonatal *Neurog1-eGFP* mice – perhaps by changing the balance among progenitor types and /or their activity within the spheres. If that is so, one might expect the behavior of the sphere-derived progeny to change following engraftment as well. We assessed whether there is a correlation between composition of the ONS and the outcome of transplantation by comparing spheres grown in LP PMA as compared to control, with respect to size of the donor-derived colonies *in situ* and/or the distribution of cell types within them.

As before, cells were isolated from mice that express GFP constitutively and cultured on ultra–low adhesion plastic with EGF, FGF–2 and either LP CM or LP PMA (collected from culture of LP_{Imm} cells grown in DMEM-10% FBS ± PMA). After 8 DIV, the ONS were harvested, dissociated, filtered, and transplanted. Enhanced neuronal production in the engrafted progenitors was assayed by using a BrdU pulse-chase approach to measure neurogenic capacity of the sphere-derived cells at 7 days after transplantation, when neurogenesis is most robust in the lesioned-recovering OE of the host(Schwob, et al., 1995). Those progeny that exit the cell cycle immediately after the BrdU pulse or after only 1 or 2 more passages through the cell cycle will retain detectable levels of BrdU at the time of tissue harvest 14 days after transplantation (which is 7 days after BrdU injection).

Examination of whole mounts in tissue harvested 14 days after transplantation indicated that both LP PMA and LP CM cultured ONS gave rise to numerous GFP(+) colonies (Fig. 7). Indeed, some of these colonies contained hundreds of cells. As a result, some of the LP CM- and LP PMA-treated colonies gave rise to GFP-labeled axon bundles that extended more than 400 μm back towards the olfactory bulb, a finding that has not been seen with ONS from base media cultures (cf. Figs. 4 and 7).

The composition of the colonies was assessed with respect to number and types of cells (as defined by morphological criteria) in cryosections through each of the colonies. The average number of cells in a colony was not significantly different between the LP CM and LP PMA conditions. However, the composition of the colonies was biased toward the production of

neurons in the LP PMA condition, and statistical analysis of the cell type distribution was significantly different between the two conditions (Chi-square = 681, p = 0.0001) (Fig. 7). When the Chi-square analysis is performed with the hypothesis that OSNs are responsible for the difference, the data are highly significant (Chi-square = 459.9, p = 0.001).

Given the large number of neurons present in the colonies derived from LP PMA–cultured ONS, label incorporation into the progenitors following BrdU pulse-chase was used to demonstrate directly that transplant derived cells were neurogenic. Sections through the donor-derived colonies were stained for GFP (to mark transplant derived cells), PGP9.5 (to mark neurons), and BrdU (to identify cells that were in S–phase when pulsed at 8 days after transplantation) (Fig. 7). Our examination revealed numerous triple-labeled, i.e., GFP(+)/PGP9.5(+)/BrdU(+), neurons, which indicates clearly that neurogenesis is occurring in transplant–derived colonies. The BrdU(+) neurons were found at all apical-to-basal level within the neuronal stratum of the OE. In some colonies, about a third to a half of the GFP(+) neurons are BrdU(+) (Fig. 7). Only a few BrdU(+)/GFP(+)/PGP9.5(−) basal cells were found – as might be expected based on the timing of BrdU incorporation relative to the rate of neurogenesis. Nonetheless, that any labeled basal cells are seen suggests that not all of the sphere-derived progenitors are exhausted during the ramp-up of neuron production in the early postnatal period, a necessary condition for a goal of maintained neuronal production.

DISCUSSION

The foundational studies presented here provide a number of key insights into the biology of olfactory stem and progenitor cells in 3-dimensional culture. We have shown that ONSs form with variable efficiency based on the status of the OE at the time of tissue harvest. GBC-like cells are present and are proliferating in ONS. Populations enriched for *Sox2eGFP*-expressing basal cells form spheres well, while populations enriched for more differentiated cells (sus cells and GBC_{INP}) do not. Immunocytochemical analyses of the ONS are in agreement with previous work using neonatal olfactory mucosa (Barraud, et al., 2007) and expand upon the transcription factor repertoire known to be expressed by cells in the spheres. Treatment of LP-derived cells by phorbol ester (PMA) conditions the media in a way that stimulates ONS to produce or retain a greater number of *Neurog1eGFP*(+) cells. Culturing epithelial progenitors as ONS creates an environment for cells that allows them to maintain the capacity to engraft appropriately, a quality shared with a previously described 3-dimensional culture model of adult olfactory epithelium (Jang, et al., 2008). On the basis of our colony forming unit/transplantation assay, spheres cultured in LP conditioned media are primed to give rise to large colonies with many neurons following engraftment. Finally, the neuronal population within the donor-derived colonies is larger when the spheres are cultured in conditioned media from PMA-treated lamina propria-derived cells.

The data are based on facile but highly quantitative assays for the growth of olfactory stem and progenitor cells in 3-dimensional structures, including the automated determination of mass, which eliminates any inconsistency due to sampling or manual image analysis, and the use of FACS to determine the numbers of specific categories of cells. With respect to the compositional analysis, the antibodies used for detection of differentiated cell types and transcription factors are standard in the field. Our lab has extensive experience with these reagents and they have been verified by the identity of staining with different antibodies generated against different peptide fragments of the protein targets. With respect to the transplantation assay, the chief technical issue that influences the interpretation of the data is the question of whether the colonies that arise in the host epithelium derive from a single engrafted stem or progenitor cell. The ONS are thoroughly dissociated and then filtered through a 35-μm mesh prior to transplantation, which prevents the engraftment of large

aggregates of cells, but does not guarantee a single cell suspension. Despite this caveat, previous work from the lab using an analogous transplantation assay argues strongly for colonies being clonally derived (Chen, et al., 2004, Goldstein, et al., 1998). The work by Chen *et al*. specifically showed that when cells from two different reporter animals (B6;129S-*Gt(ROSA)26Sor* and C57BL/6-Tg(CAG-EGFP)1Osb/S) are mixed prior to transplantation, colonies containing both GFP(+) and LacZ(+) cells are never seen, which provides strong evidence of clonality.

Cellular composition of spheres and implications

The analysis of various antigens and markers of differentiation or proliferation in ONS indicates that spheres contain a mixture of both differentiated cells – HBCs, duct/gland cells, sus cells, neurons, and GBC-like progenitors. The composition appears to be biased against HBCs as CK14(+) cells are rare by comparison with the aggregate population of Sox2(+), *Sox2eGFP*(+) or EdU/Ki67(+) cells, all of which are GBC-like. It may be the case that HBCs are disadvantaged during the early assembly and growth of the spheres because they usually adhere to the basal lamina(Holbrook, et al., 1995). More specifically, HBCs are known to express integrins, and various cells types have been shown to undergo anoikis after loss of integrin mediated adhesion (Carter, et al., 2004, Frisch and Ruoslahti, 1997).

It was something of a surprise to note the differences between the expression of Sox2 protein and GFP driven from the Sox2 locus in the spheres. Sox2 protein is expressed in a small percentage of cells, but GFP is present in an overwhelming majority of cells in the spheres derived from the neonatal *ΔSox2eGFP* mice. In this case, the extended half life of GFP acts like a short–term lineage tracer, suggesting that most cells in the spheres expressed Sox2 at one time, but have either differentiated down a neuronal pathway or ceased expression from the locus due to a lack of proper signals (or presence of inhibitors) that would maintain Sox2 expression and therefore an expansive progenitor state. The presence of cells with markers of neuronal differentiation (neuron-specific tubulin and NCAM) at the time points examined (7-11 DIV) suggests that neurogenesis is ongoing in the ONS because olfactory sensory neurons normally undergo apoptosis within a very few days of denervation (Michel, et al., 1994, Schwartz Levey, et al., 1991, Schwob, et al., 1992). Therefore, any TuJ(+) or NCAM(+) cells likely arose during the culture period or were presented with a unique set of survival signals in ONS culture.

Sphere forming capacity

The results presented here have defined ONS-forming capacity as a function of the proliferative state of the epithelium from which it is derived and of the specific cell types used to initiate ONS generation. We did not directly test whether spheres can arise from a single cell, as that question is better assayed by passaging. The finding that most ONS are heterogenous and complex suggests the formation of an ONS may require such complexity, echoing the results seen in air-liquid interface cultures (Jang, et al., 2008). Indeed, the cultures of sorted cells are very consistent with that interpretation. Immediate neuronal precursors (GBC_{INP}), the most downstream of the GBC progenitor populations, produce only neurons *in vivo* (Packard et al, 2010). It follows that *Neurog1eGFP*(+) cells, which correspond to GBC_{INP} cells and their recent neuronal progeny, are effectively unable to generate the necessary complexity *in vitro* and form ONSs. In contrast, multipotent GBC progenitors (GBC_{MPP}) are able to produce multiple cell types in the spheres and thus, give rise to heterogeneity *in vivo* following engraftment. Thus, *ΔSox2eGFP*(+low) cells (which include GBC_{MPP} and some HBCs) are capable of producing ONS – presumably because they retain the capacity to generate the appropriate complexity and heterogeneity. When the data on ONS formation from sorted cells are taken together with the retained capacity for engraftment and multi-lineage differentiation after transplantation, then the formation of

spheres in non-adherent cultures correlates with and seems to mark the retention of multipotency in this system.

Inability to passage

Given the dramatic expansive growth early in the culture period of ONS and the remarkable capacity of what are likely to be single sphere-derived cells to generate colonies containing many hundreds of cells after transplantation, it is perhaps surprising that we and the field have been unsuccessful in passaging neonatal ONS (Barraud, et al., 2007). The observed plateau of mass expansion during the later time points suggests a few obvious possibilities: 1) the growth of spheres and the cellular milieu created by their increased diameter compromises further proliferation and expansion, 2) the proliferative capacity of cells in ONS is exhausted by progression, or blocked by an absence of needed signals, or reaches equilibrium with cell death around 7 DIV. Attempts at passaging spheres to reinvigorate growth were unsuccessful suggesting that the first possibility is unlikely to be responsible. However, of the second set of explanations for the failure to progress, exhaustion of progenitor capacity is not consistent with the capacity for substantial expansion *in vivo* and suggests that there are signals, yet to be discovered, that will push growth and allow passaging.

The restrictions of ONS growth and passaging contrast with the apparent lack of such limitations when culturing neurospheres from CNS, where sphere formation and extensive passaging have been shown to correlate with multilineage differentiation capacity and stem cell-like behavior (Louis, et al., 2008, Reynolds and Weiss, 1992, Reynolds and Weiss, 1996). The data for ONS presented here show that some cells which have characteristics of multipotent progenitors and stem cells *in vivo* are present in the ONSs, but it appears that these cells are not receiving the proper cues *in vitro* required to recapitulate the remarkable capacity of these cells *in vivo*.

It is of interest that other groups have reported the ability to passage free floating spheres from human nasal mucosa (Murrell, et al., 2005) and mouse embryonic mucosa (Tome, et al., 2009). The reported ability to passage these spheres suggests that there may be some intrinsic differences in the cell types present or signals required to maintain these cells in an expansive and proliferative state. The article by Tome and colleagues describes two morphologic types of spheres from embryonic olfactory mucosa: Type I, which are spherical, resemble CNS neurospheres, and express nestin; and Type II, which are described as more irregular, with limited proliferative and expansive capacity, and extensive cytokeratin positivity (Tome, et al., 2009). In contrast, we find that the majority of ONS derived from neonates appear to be solid, with a slightly more opaque center as they increase in diameter. These have features in common with both types described by Tome et al (2009). The rare ONS with a hollow center that we also see and describe above may more clearly correspond to the Type II spheres described by Tome *et. al* from the embryonic olfactory mucosa. Ultimately, the different time of origin may be responsible for the qualitative and functional differences seen in the two models.

Influences of the lamina propria

The current work contributes additional data to an ever increasing body of literature that demonstrates the importance of reciprocal signals between epithelium and stroma in various tissues. Much of the work describing these effects in the olfactory mucosa has been performed in embryonic animals and explants of embryonic tissue (LaMantia, et al., 2000, Rawson, et al., 2010, Tucker, et al., 2010). Our work demonstrates that an immortalized cell line generated from adult lamina propria has a significant impact on sphere composition. Our lab is actively pursuing a proteomic analysis of the factors produced by the LP_{Imm} cells,

with and without stimulation by PMA. It is of special interest that neuregulin1 – a prominent component of many stroma-derived media – is known to be expressed in the OE (Salehi-Ashtiani and Farbman, 1996) and is found in LP_{Imm}-conditioned media (Woochan Jang and James E. Schwob, unpublished data). PMA has been shown to stimulate the release of neuregulin1 from 3T3 fibroblasts, making this factor a likely candidate for the effects we are observing (Montero, et al., 2000, Salehi-Ashtiani and Farbman, 1996). Likewise, studies in lung have shown that neuregulin mediates interactions between stroma and epithelium that regulate epithelial cell differentiation(Dammann, et al., 2003).

The enhanced population of GFP(+) cells found in spheres that are cultured in LP PMA media suggests another possible factor that could be acting on the neuronal progenitors or immature neurons in ONS, namely hepatocyte growth factor (HGF). HGF is released in response to PMA treatment of fibroblasts, is known to inhibit anoikis in epithelial–derived cells, and is also expressed in the lamina propria of the olfactory mucosa (Gohda, et al., 1992, Thewke and Seeds, 1996, Zeng, et al., 2002). The demonstration that the LP_{Imm} cells retain the capacity to secrete factors that direct cell fate or neuronal survival suggests that cells in the lamina propria of the normal adult may be releasing factors *in vivo* that influence neuronal differentiation or survival.

Translational prospects

The transplant assay allows us to test the progenitor cell capacity of ONS and assess whether there is a correlation between their composition and the outcome of their transplantation. That *in vitro* influences on cell fate and differentiation, such as the enhancing effects of LP PMA, are reflected in the outcome following transplantation suggests that *in vitro* manipulations of ONSs can have dramatic effects on engraftment outcomes. Our results have translational implications. The feasibility of using any transplantation of any stem or progenitor cell population as a therapeutic moiety necessitates control over expansion, cell fate, and differentiation, such that the donor cells are primed to generate the desired cell types upon transplantation. That manipulating a particular cell population *in vitro* carries over and is perpetuated in the resultant colony demonstrates clearly that studies modulating the process of sphere formation have the potential to inform and predict the behavior of these cells after transplantation.

Supplementary Material

Refer to Web version on PubMed Central for supplementary material.

Acknowledgments

The authors thank Adam Packard for his help with producing virus for immortalization of the LP cells and Po Kwok-Tse for her outstanding technical assistance. The authors also thank the Schwob lab for helpful discussions about the data and manuscript. This work was supported by grants from the NIH to J.E.S. (RO1 DC002167), and to R.C.K. (F30 DC010276).

ABBREVIATIONS

CK	cytokeratin (used interchangeably with keratin)
CM	conditioned media
FACS	fluorescence activated cell sorting
FGF	fibroblast growth factor
GBC	globose basal cell

HBC	horizontal basal cell
IHC	immunohistochemistry
LP	lamina propria
MeBr	methyl bromide
NCAM	neural cell adhesion molecule
OE	olfactory epithelium
OM	olfactory mucosa
ONS	olfactory neurosphere
OSN	olfactory sensory neuron
PECAM	platelet endothelial cell adhesion molecule
PMA	phorbol ester (phorbol-12-myristate-13-acetate, a.k.a. TPA)
PND	post-natal day
Sus	sustentacular cell

REFERENCES

1. Amos S, Martin PM, Polar GA, Parsons SJ, Hussaini IM. Phorbol 12-myristate 13-acetate induces epidermal growth factor receptor transactivation via protein kinase Cdelta/c-Src pathways in glioblastoma cells. J Biol Chem. 2005; 280:7729–7738. [PubMed: 15618223]
2. Barraud P, He X, Zhao C, Ibanez C, Raha-Chowdhury R, Caldwell MA, Franklin RJ. Contrasting effects of basic fibroblast growth factor and epidermal growth factor on mouse neonatal olfactory mucosa cells. Eur J Neurosci. 2007; 26:3345–3357. [PubMed: 18088275]
3. Carter LA, MacDonald JL, Roskams AJ. Olfactory horizontal basal cells demonstrate a conserved multipotent progenitor phenotype. J Neurosci. 2004; 24:5670–5683. [PubMed: 15215289]
4. Chen X, Fang H, Schwob JE. Multipotency of purified, transplanted globose basal cells in olfactory epithelium. J Comp Neurol. 2004; 469:457–474. [PubMed: 14755529]
5. Dammann CE, Nielsen HC, Carraway KL 3rd. Role of neuregulin-1 beta in the developing lung. Am J Respir Crit Care Med. 2003; 167:1711–1716. [PubMed: 12663324]
6. DeHamer MK, Guevara JL, Hannon K, Olwin BB, Calof AL. Genesis of olfactory receptor neurons in vitro: regulation of progenitor cell divisions by fibroblast growth factors. Neuron. 1994; 13:1083–1097. [PubMed: 7946347]
7. Dontu G, Abdallah WM, Foley JM, Jackson KW, Clarke MF, Kawamura MJ, Wicha MS. In vitro propagation and transcriptional profiling of human mammary stem/progenitor cells. Genes Dev. 2003; 17:1253–1270. [PubMed: 12756227]
8. Ellis P, Fagan BM, Magness ST, Hutton S, Taranova O, Hayashi S, McMahon A, Rao M, Pevny L. SOX2, a persistent marker for multipotential neural stem cells derived from embryonic stem cells, the embryo or the adult. Dev Neurosci. 2004; 26:148–165. [PubMed: 15711057]
9. Frisch SM, Ruoslahti E. Integrins and anoikis. Curr Opin Cell Biol. 1997; 9:701–706. [PubMed: 9330874]
10. Gohda E, Kataoka H, Tsubouchi H, Daikilara Y, Yamamoto I. Phorbol ester-induced secretion of human hepatocyte growth factor by human skin fibroblasts and its inhibition by dexamethasone. FEBS Lett. 1992; 301:107–110. [PubMed: 1451778]
11. Goldstein BJ, Fang H, Youngentob SL, Schwob JE. Transplantation of multipotent progenitors from the adult olfactory epithelium. Neuroreport. 1998; 9:1611–1617. [PubMed: 9631475]
12. Gong S, Zheng C, Doughty ML, Losos K, Didkovsky N, Schambra UB, Nowak NJ, Joyner A, Leblanc G, Hatten ME, Heintz N. A gene expression atlas of the central nervous system based on bacterial artificial chromosomes. Nature. 2003; 425:917–925. [PubMed: 14586460]

13. Gordon MK, Mumm JS, Davis RA, Holcomb JD, Calof AL. Dynamics of MASH1 expression in vitro and in vivo suggest a non-stem cell site of MASH1 action in the olfactory receptor neuron lineage. Mol Cell Neurosci. 1995; 6:363–379. [PubMed: 8846005]

14. Guo Z, Packard A, Krolewski RC, Manglapus GL, Harris M, Schwob JE. Expression of Pax6 and Sox2 in Adult Olfactory Epithelium. Journal of Comparative Neruology x. 2010

15. Holbrook EH, Szumowski KE, Schwob JE. An immunochemical, ultrastructural, and developmental characterization of the horizontal basal cells of rat olfactory epithelium. J Comp Neurol. 1995; 363:129–146. [PubMed: 8682932]

16. Holbrook EL, Leopold D, Schwob JE. A description of axonal abnormalities observed in human olfactory epithelium. Chem Senses. 2003; 28 in press.

17. Huard JM, Youngentob SL, Goldstein BJ, Luskin MB, Schwob JE. Adult olfactory epithelium contains multipotent progenitors that give rise to neurons and non-neural cells. J Comp Neurol. 1998; 400:469–486. [PubMed: 9786409]

18. Iwai N, Zhou Z, Roop DR, Behringer RR. Horizontal basal cells are multipotent progenitors in normal and injured adult olfactory epithelium. Stem Cells. 2008; 26:1298–1306. [PubMed: 18308944]

19. Jang W, Kim KP, Schwob JE. Nonintegrin laminin receptor precursor protein is expressed on olfactory stem and progenitor cells. J Comp Neurol. 2007; 502:367–381. [PubMed: 17366606]

20. Jang W, Lambropoulos J, Woo JK, Peluso CE, Schwob JE. Maintaining epitheliopoietic potency when culturing olfactory progenitors. Exp Neurol. 2008; 214:25–36. [PubMed: 18703052]

21. Jang W, Lambropoulos J, Woo JK, Peluso CE, Schwob JE. Maintaining epitheliopoietic potency when culturing olfactory progenitors. Journal of Experimental Neurology. 2008

22. Krause DS, Theise ND, Collector MI, Henegariu O, Hwang S, Gardner R, Neutzel S, Sharkis SJ. Multi-organ, multi-lineage engraftment by a single bone marrow-derived stem cell. Cell. 2001; 105:369–377. [PubMed: 11348593]

23. LaMantia AS, Bhasin N, Rhodes K, Heemskerk J. Mesenchymal/epithelial induction mediates olfactory pathway formation. Neuron. 2000; 28:411–425. [PubMed: 11144352]

24. Leung CT, Coulombe PA, Reed RR. Contribution of olfactory neural stem cells to tissue maintenance and regeneration. Nat Neurosci. 2007; 10:720–726. [PubMed: 17468753]

25. Louis SA, Rietze RL, Deleyrolle L, Wagey RE, Thomas TE, Eaves AC, Reynolds BA. Enumeration of neural stem and progenitor cells in the neural colony-forming cell assay. Stem Cells. 2008; 26:988–996. [PubMed: 18218818]

26. Michel D, Moyse E, Brun G, Jourdan F. Induction of apoptosis in mouse [correction of rat] olfactory neuroepithelium by synaptic target ablation. Neuroreport. 1994; 5:1329–1332. [PubMed: 7919191]

27. Montero JC, Yuste L, Diaz-Rodriguez E, Esparis-Ogando A, Pandiella A. Differential shedding of transmembrane neuregulin isoforms by the tumor necrosis factor-alpha-converting enzyme. Mol Cell Neurosci. 2000; 16:631–648. [PubMed: 11083924]

28. Mumm JS, Shou J, Calof AL. Colony-forming progenitors from mouse olfactory epithelium: evidence for feedback regulation of neuron production. Proc Natl Acad Sci U S A. 1996; 93:11167–11172. [PubMed: 8855327]

29. Murphy C. The chemical senses and nutrition in older adults. J Nutr Elder. 2008; 27:247–265. [PubMed: 19042574]

30. Murrell W, Feron F, Wetzig A, Cameron N, Splatt K, Bellette B, Bianco J, Perry C, Lee G, Mackay-Sim A. Multipotent stem cells from adult olfactory mucosa. Dev Dyn. 2005; 233:496–515. [PubMed: 15782416]

31. Naessen R. An enquiry on the morphological characteristics and possible changes with age in the olfactory region of man. Acta Otolaryngol. 1971; 71:49–62. [PubMed: 5100075]

32. Nakashima T, Kimmelman CP, Snow JB Jr. Structure of human fetal and adult olfactory neuroepithelium. Arch Otolaryngol. 1984; 110:641–646. [PubMed: 6477257]

33. Okabe M, Ikawa M, Kominami K, Nakanishi T, Nishimune Y. 'Green mice' as a source of ubiquitous green cells. FEBS Lett. 1997; 407:313–319. [PubMed: 9175875]

34. Othman MM, Klueber KM, Roisen FJ. Identification and culture of olfactory neural progenitors from GFP mice. Biotech Histochem. 2003; 78:57–70. [PubMed: 14533842]

35. Pixley SK, Bage M, Miller D, Miller ML, Shi M, Hastings L. Olfactory neurons in vitro show phenotypic orientation in epithelial spheres. Neuroreport. 1994; 5:543–548. [PubMed: 8025240]
36. Purton LE, Scadden DT. Limiting factors in murine hematopoietic stem cell assays. Cell Stem Cell. 2007; 1:263–270. [PubMed: 18371361]
37. Rawson NE, Lischka FW, Yee KK, Peters AZ, Tucker ES, Meechan DW, Zirlinger M, Maynard TM, Burd GB, Dulac C, Pevny L, LaMantia AS. Specific mesenchymal/epithelial induction of olfactory receptor, vomeronasal, and gonadotropin-releasing hormone (GnRH) neurons. Dev Dyn. 2010; 239:1723–1738. [PubMed: 20503368]
38. Reynolds BA, Weiss S. Generation of neurons and astrocytes from isolated cells of the adult mammalian central nervous system. Science. 1992; 255:1707–1710. [PubMed: 1553558]
39. Reynolds BA, Weiss S. Clonal and population analyses demonstrate that an EGF-responsive mammalian embryonic CNS precursor is a stem cell. Dev Biol. 1996; 175:1–13. [PubMed: 8608856]
40. Salehi-Ashtiani K, Farbman AI. Expression of neu and Neu differentiation factor in the olfactory mucosa of rat. Int J Dev Neurosci. 1996; 14:801–811. [PubMed: 9010726]
41. Sato T, Vries RG, Snippert HJ, van de Wetering M, Barker N, Stange DE, van Es JH, Abo A, Kujala P, Peters PJ, Clevers H. Single Lgr5 stem cells build crypt-villus structures in vitro without a mesenchymal niche. Nature. 2009; 459:262–265. [PubMed: 19329995]
42. Schwartz Levey M, Chikaraishi DM, Kauer JS. Characterization of potential precursor populations in the mouse olfactory epithelium using immunocytochemistry and autoradiography. J Neurosci. 1991; 11:3556–3564. [PubMed: 1719164]
43. Schwob JE, Szumowski KE, Stasky AA. Olfactory sensory neurons are trophically dependent on the olfactory bulb for their prolonged survival. J Neurosci. 1992; 12:3896–3919. [PubMed: 1403089]
44. Schwob JE, Youngentob SL, Meiri KF. On the formation of neuromata in the primary olfactory projection. J Comp Neurol. 1994; 340:361–380. [PubMed: 8188856]
45. Schwob JE, Youngentob SL, Mezza RC. Reconstitution of the rat olfactory epithelium after methyl bromide-induced lesion. J Comp Neurol. 1995; 359:15–37. [PubMed: 8557844]
46. Shackleton M, Vaillant F, Simpson KJ, Stingl J, Smyth GK, Asselin-Labat ML, Wu L, Lindeman GJ, Visvader JE. Generation of a functional mammary gland from a single stem cell. Nature. 2006; 439:84–88. [PubMed: 16397499]
47. Shou J, Murray RC, Rim PC, Calof AL. Opposing effects of bone morphogenetic proteins on neuron production and survival in the olfactory receptor neuron lineage. Development. 2000; 127:5403–5413. [PubMed: 11076761]
48. Shou J, Rim PC, Calof AL. BMPs inhibit neurogenesis by a mechanism involving degradation of a transcription factor. Nat Neurosci. 1999; 2:339–345. [PubMed: 10204540]
49. Thewke DP, Seeds NW. Expression of hepatocyte growth factor/scatter factor, its receptor, c-met, and tissue-type plasminogen activator during development of the murine olfactory system. J Neurosci. 1996; 16:6933–6944. [PubMed: 8824331]
50. Tome M, Lindsay SL, Riddell JS, Barnett SC. Identification of nonepithelial multipotent cells in the embryonic olfactory mucosa. Stem Cells. 2009; 27:2196–2208. [PubMed: 19544421]
51. Tucker ES, Lehtinen MK, Maynard T, Zirlinger M, Dulac C, Rawson N, Pevny L, Lamantia AS. Proliferative and transcriptional identity of distinct classes of neural precursors in the mammalian olfactory epithelium. Development. 2010; 137:2471–2481. [PubMed: 20573694]
52. Woodward WA, Chen MS, Behbod F, Rosen JM. On mammary stem cells. J Cell Sci. 2005; 118:3585–3594. [PubMed: 16105882]
53. Zeng Q, Chen S, You Z, Yang F, Carey TE, Saims D, Wang CY. Hepatocyte growth factor inhibits anoikis in head and neck squamous cell carcinoma cells by activation of ERK and Akt signaling independent of NFkappa B. J Biol Chem. 2002; 277:25203–25208. [PubMed: 11994287]

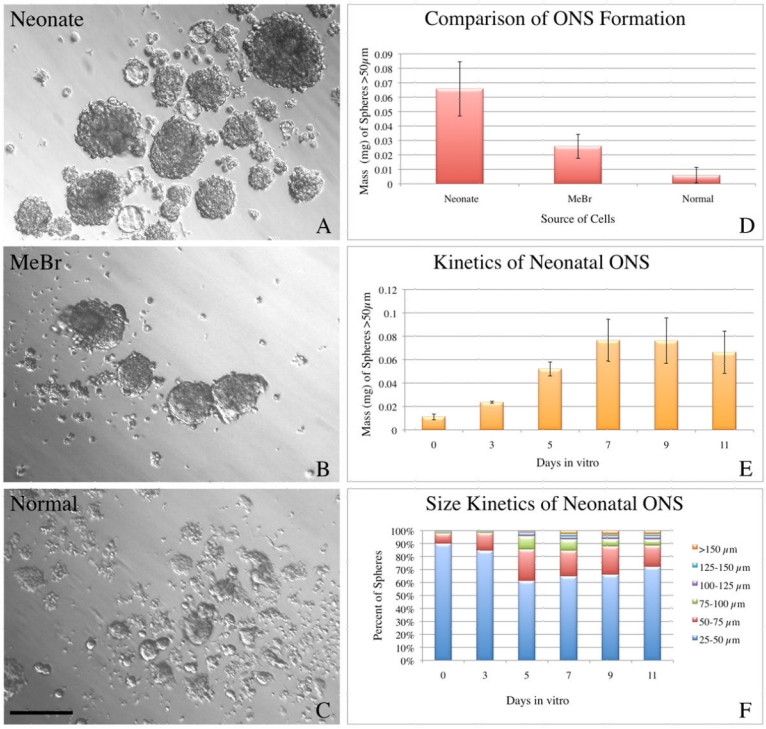

Figure 1. Neonatal olfactory mucosa forms spheres most efficiently

A-C) ONS were generated from three different source tissues: neonates (**A**), adult animals 2 days after methyl bromide lesion (**B**), and normal adult animals (**C**). All three conditions result in detectable sphere formation as seen by representative bright field images (**A-C**). **D)** At 7 DIV, plots of the average mass ± SEM demonstrate that ONS derived from neonates are most spherogenic, followed by ONS derived from MeBr–lesioned adults. Normal epithelium produces very few ONS. ANOVA indicates significant variation across conditions ($F = 9.167$, $p = 0.0085$) and a Tukey–Kramer Multiple Comparisons Test indicates that neonatal ONS were significantly different from normal adult ONS ($q = 5.777$, $p < 0.01$). **E)** Neonatal ONS undergo rapid expansion early *in vitro* and mass expansion plateaus around 7–9 DIV. Parallel aliquots of cells were established and mass ± SEM was measured at the indicated time points to establish a growth curve for neonatal ONS. **F)** The percent of ONS in progressively larger size bins was plotted as a function of time *in vitro*. The data show that ONS increase in size and the size distribution changes over the culture period. Scale bar in **C** is 100 μm and applies to **A–C**.

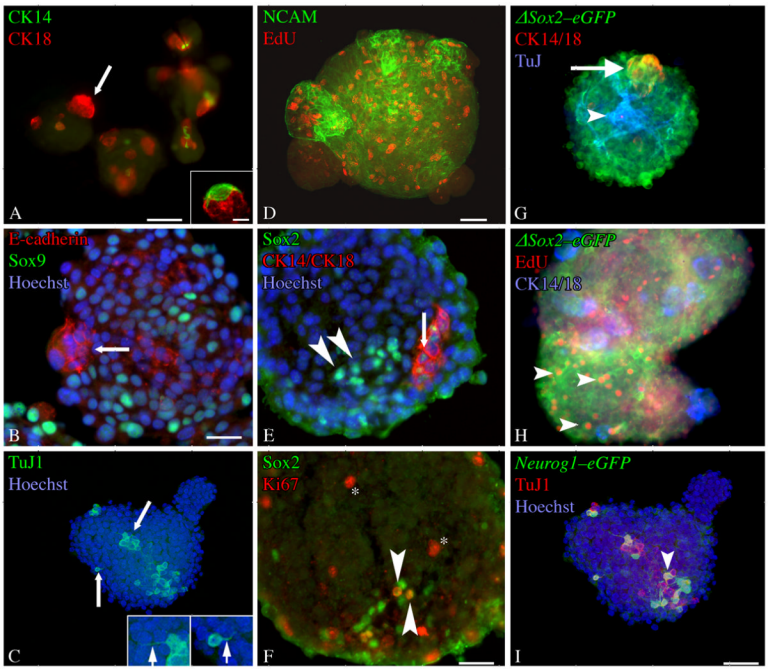

Figure 2. Olfactory neurospheres express cell-type specific markers characteristic of intact olfactory epithelium

ONS were stained as whole mounts (A-D) or cryosectioned and stained as described (E–F). **A**) Occasional CK14(+) cells can be found in ONS, but they appear with less frequency than any other differentiated cell type examined. Some of the CK14(+) cells have morphologies highly reminiscent of the *in vivo* HBC counterparts (inset). CK18(+) cells are also present in the spheres and are distinct from CK14(+) cells. These often occur in subdomains that appear as “buds” of morphologically homogeneous cells (arrow). **B)** Staining for E-cadherin, a marker of sus and Bowman's Duct and Gland structures *in vivo*, also labels these subdomains (arrow). Numerous Sox9(+) cells, a marker of Bowman's Duct and Gland cells in the OE, are present in ONSs. **C)** TuJ-1(+) cells are found throughout ONSs. Often, these cells have processes (arrows–shown at higher power in insets) that resemble axons (left inset) or apical dendrites (right inset). **D)** NCAM(+) also labels a neuronal population present in ONS. EdU(+) cells indicate that DNA synthesis is actively occuring in the ONSs. **E)** Sox2(+)/CK14(−)/CK18(−) cells (arrowheads) and Sox2(+)/CK14(+)/CK18(+) cells (arrow) are found in ONSs. **F)** A number of Sox2(+) cells are Ki67(+) (arrowheads). Additional cells in the ONSs are also Ki67(+) (asterisk). **G, H)** ONSs derived from *ΔSox2eGFP* neonates The vast majority of cells in the spheres are GFP(+). These include both cytokeratin 14/18(+) cells (arrow) found in subdomains and TuJ-1(+) cells stretching throughout the ONS (arrowhead). **H**) Many of the GFP(+) cells are also EdU(+) and cytokeratin 14/18 (−) (arrowheads). These criteria define GBCs *in vivo* and indicate their presence in ONSs. Separate CK14 and CK18 antibodies were visualized with secondary antibodies conjugated to the same flourophore to allow for detection of additional antigens (TuJ in **G**, EdU in **H**). **I)** ONSs derived from *Neurog1eGFP* neonates. A number of cells in the spheres are GFP(+) and many of these are TuJ1 (+) and/or PGP9.5(+) (arrowheads). Scale bar in **A** is 50 μm. Scale bar in the inset of **A** is 10 μm. Scale bar in **B** is 25 μm and applies to **B** and **E**. Scale bar in **D** is 50 μm and applies to **C** and **D**. Scale bar in **F** is 25 μm. Scale bar in **I** is 50 μm and applies to **G** and **H**.

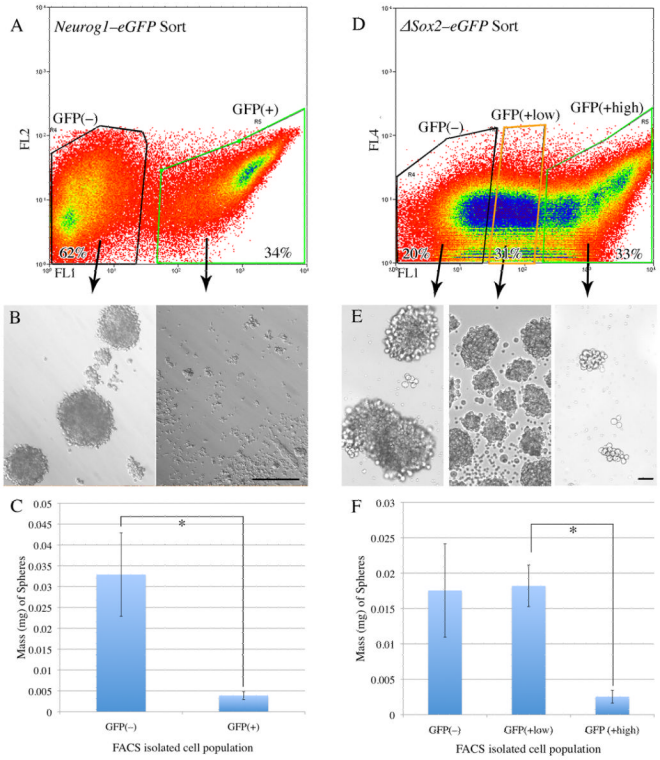

Figure 3. *Neurog1eGFP*(+) cells do not form olfactory neurospheres, while a subset of *ΔSox2eGFP*(+) cells do

A) *Neurog1eGFP* neonatal OE was dissociated and sorted into GFP(−) and GFP(+) fractions (62% and 34% of cells, respectively). Cells were gated on forward scatter/side scatter and pulse width to restrict the sort to single cells. Cells were also gated as propidium iodide negative (PI[−]) indicating viability. The cells were then cultured under ONS–forming conditions. **B**) Brightfield examination of the two different sorted populations from *Neurog1eGFP* neonates at 7 DIV demonstrates ONS formation in the GFP(−) population and negligible ONS formation in the GFP(+) population. **C)** Quantitative analysis of the two different *Neurog1eGFP* sorted populations at 7 DIV indicates that the mass of spheres formed by the GFP(−) population is more than four–fold greater than the mass derived from the GFP(+) population ($p = 0.0313$, Wilcoxon matched–pairs signed–ranks test). **D**) *ΔSox2eGFP* neonatal OE was dissociated and sorted into GFP(no), GFP(low), and GFP(high) populations (20%, 31%, and 33% of PI(−) cells, respectively). **E**) Brightfield examination of the cultures from the three different sorted populations at 7 DIV demonstrates robust ONS formation in the GFP(low) and GFP(no) populations, but poor ONS formation in the GFP(high) population. **F**) Quantitative analysis of sphere formation from the three different *ΔSox2eGFP* sorted populations at 7 DIV indicates that the mass of spheres from the GFP(low) population is approximately four-fold greater than the mass of the GFP(high) population (Kruskal-Wallis, KW = 7.848, $p= 0.0009$, Dunn's multiple comparisons test for GFP(high) vs. GFP(low), $p < 0.05$).

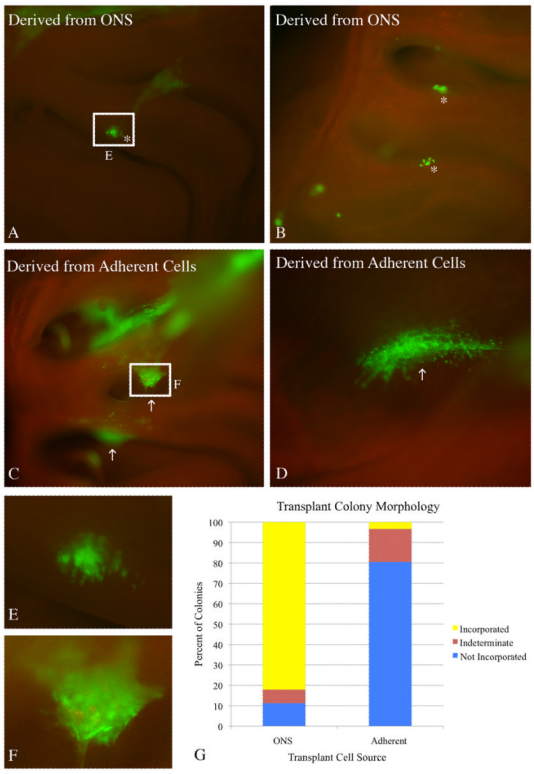

Figure 4. ONS-derived cells engraft appropriately into the lesioned recovering epithelium

Cells derived from 8 DIV ONS were compared to cells derived from 8 DIV adherent cultures in a transplantation assay that tests engraftment capacity. **A**, **B**) 2 weeks after transplantation, cells derived from ONS cultures formed primarily smaller colonies that have incorporated and integrated into the regenerating epithelium (asterisks). **C**, **D**) In contrast, cells derived from adherent cultures formed primarily large, sprawling colonies (arrows) that have not incorporated into the OE of methyl bromide-lesioned host animals. The colonies appear to sit above the epithelium or bridge adjacent areas of epithelium via synechiae. **E)** Inset of boxed region in **A** shows more detailed morphology of an ONS–derived colony. The GFP(+) cells intercalate extensively with host cells as seen by the punctate GFP signal intermixed with GFP(−) host cells, suggesting appropriate incorporation into the epithelium. **F)** Inset of boxed region in **C** shows more detailed morphology of an adherent culture–derived colony. The GFP(+) cells do not intercalate extensively with host cells. **G)** Engrafted colonies from three host animals for each transplant condition were classified into three categories: (1) incorporated (resembling the colonies identified by asterisks) – depicted in yellow; (2) not incorporated (resembling the colonies identified by arrows) – depicted in blue; or (3) undefined (unable to definitively classify) – depicted in plum. The graph clearly shows that colonies resulting from ONS-derived cells result in a higher percentage of incorporated colonies. Yates Chi-square analysis of the raw data indicates a significant difference between the two conditions (Yates Chi-square = 36.999, Yates p-value = 1×10^{-8}).

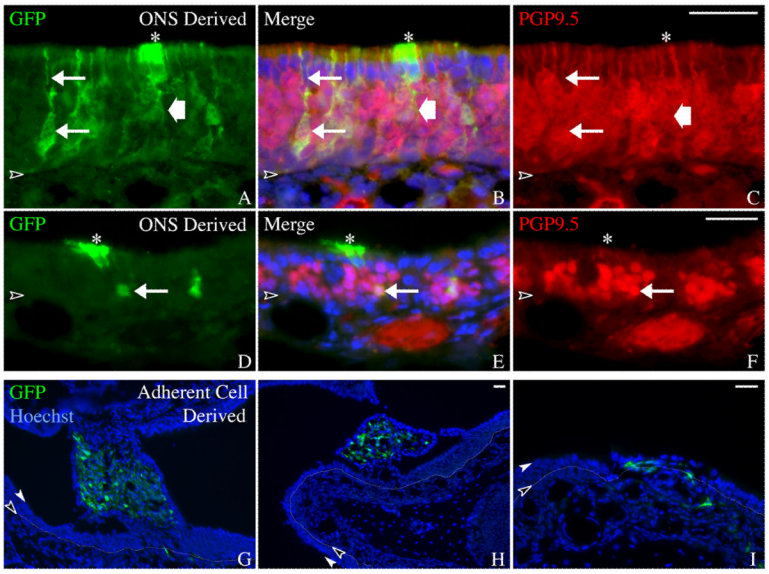

Figure 5. ONS-derived colonies contain cell types that resemble adjacent host OE

A-F) Coronal sections of ONS-derived colonies confirm whole mount observations that the sphere-derived cells intergrate into the regenerating epithelium. Neurons (arrows) and sustentacular cells (asterisks) are identified based on morphology and immunostaining. GFP(+)/PGP9.5(+) neurons with an apical dendrite (upper arrow in **A**-**C**) are seen in the transplant-derived colonies. Transplant-derived sustentacular cells (asterisks) are identified as GFP(+)/PGP9.5(−) cells with apically positioned nuclei and footprocesses extending toward the basal lamina (wide arrow). Scale bar in **C** is 25 μm and applies to **A**-**C**. Scale bar in **F** is 25 μm and applies to **D**-**F**. **G**-**I**) Coronal sections of adherent culture–derived colonies confirm whole mount observations that these cells do not incorporate appropriately into regenerating epithelium. Endogenous GFP was compared with Hoechst labeling of all nuclei. The colonies resulting from adherent culture–derived cells appear spindle-shaped and mesenchymal and thus, are distinct morphologically from the normal differentiated cell types found in the OE. The basal lamina is designated by a black arrowhead and thin dotted line, the apical surface of the epithelium is designated by a white arrowhead. Scale bar in **H** is 25 μm and applies to **G**. Scale bar in **I** is 25 μm.

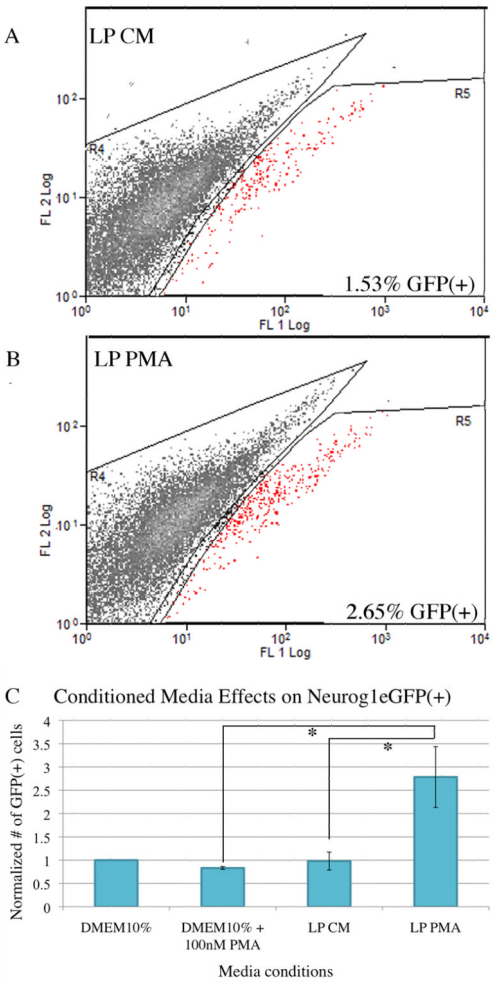

Figure 6. Culturing in LP PMA media increases the percentage of GFP(+) cells in ONS derived from *Neurog1eGFP* neonates

Cells derived from *Neurog1eGFP* neonates and cultured as ONS for 7 DIV show increased GFP(+) cells after culture in conditioned media from phorbol ester-treated LP_{Imm} cells (LP PMA). Dissociated ONS at 7 DIV were assayed for the percentage of GFP(+) cells by flow cytometry. **A**, **B)** Representative FACS profiles of dissociated cells from ONS cultured in control conditioned media (LP CM, panel **A**) and LP PMA (panel **B**). ONS cultured in LP PMA consistently and reproducibly showed an increased percentage of GFP(+) cells by flow cytometry. GFP(+) cells are depicted as red spots on the FACS profiles. Both profiles were equivalently gated for single cells and exclusion of propidium iodide. **C**) The number of GFP(+) cells from base media (DMEM10%), base media treated with phorbol ester (DMEM10% + 100 nM PMA), conditioned media from LP_{Imm} cells (LP CM), and conditioned media from phorbol ester treated (100 nM) LP_{Imm} cells (LP PMA) were normalized to base media for each replicate and the average normalized number of GFP(+) cells was plotted for each condition. Raw percentage values for each group varied significantly across the conditions (repeated measures ANOVA, $F = 4.153$, $p = 0.0014$) and LP PMA was significantly different from LP CM and DMEM10% + 100 nM PMA by Tukey-Kramer post tests ($q = 5.474$, $p < 0.05$; $q = 5.963$, $p < 0.001$, respectively).

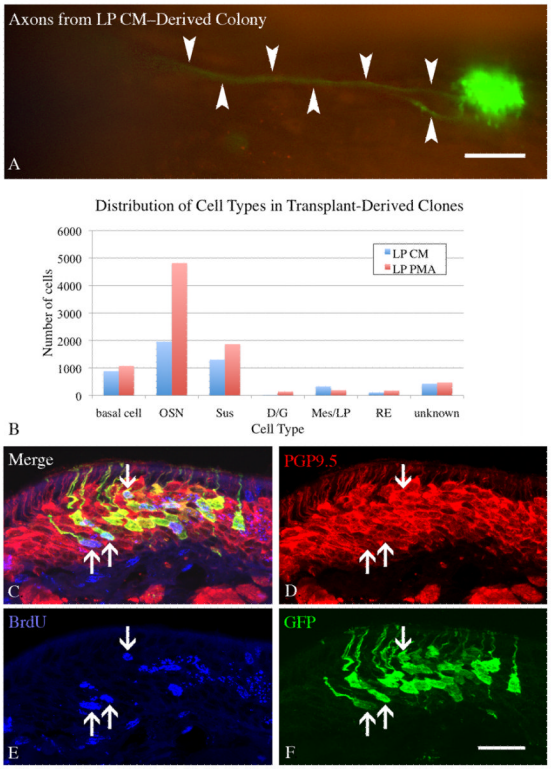

Figure 7. Colonies derived from spheres cultured in LP PMA have an increased number of neurons

ONS derived from constitutively expressing GFP donor neonates were cultured in LP CM or LP PMA for 8 DIV, then dissociated and transplanted into 1 day post methyl bromide-lesioned host animals. Animals were sacrificed 2 weeks after transplantation and screened for GFP(+) donor-derived colonies. **A)** Large colonies were seen in both conditions (LP CM shown here), with some having visible axons projecting back towards the olfactory bulb (arrow). Scale bar is 100 μm. **B)** All colonies from LP CM and LP PMA hosts (n=3 per condition), were counted and the cell types present were documented. Chi–square analysis indicates that the two distributions are significantly different from one another (Chi–square = 681, $p < 0.0001$) and neurons significantly contribute to this difference (Chi–square = 459.9, $p < 0.001$). **C-F)** A cohort of host mice were pulsed with 30 mg/kg BrdU 8 days after transplantation to label cells in S-phase and then allowed to survive for an additional 6 days (the chase phase) before fixation. Many neurons arise *in vivo* from transplant-derived cells (arrows) as shown by co-labeling with GFP to identify donor–derived cells, PGP9.5 to identify neurons, and BrdU to identify cells labeled during the pulse. Scale bar in **F** is 25 μm applies to **C**-**F**.

Table 1

Antibodies used in the study

Primary antibody	Source and catalog number	Immunogen and preparation	Specificity	Cell Types Stained
Chicken α–GFP	AbCam ab13970	Recombinant full-length protein. This anti-GFP antibody recognizes the enhanced form of GFP, and all of the fluorescent proteins made by this algae, including yellow FP.	Antibody stains various transgenic reporter mice bearing a GFP transgene, it does not stain wild type littermates.	GFP-labeled cells from *ΔSox2-eGFP* heterozygous mice, *Neurog1-eGFP* BAC transgenic mice, or constitutive GFP-expressing mice
Rabbit α–GFP	AbCam ab6556	Highly purified recombinant full length GFP made in *Escherichia coli*	Antibody stains various transgenic reporter mice bearing a GFP transgene, it does not stain wild type littermates.	GFP-labeled cells from *ΔSox2-eGFP* heterozygous mice, *Neurog1-eGFP* BAC transgenic mice, or constitutive GFP-expressing mice
Goat α–Sox2	Santa Cruz, sc-17320	Amino acids 277-293 of human Sox2 affinity-purified. YLPGAEVPEPAAPSRLH	Monospecific, reacting with a 34 kDa band in WB of mouse and human ES cell lysates	Sustentacular cells, HBCs and several subsets of GBCs
Rabbit α–Sox9	Chemicon (Millipore) AB5535	Synthetic peptide from human Sox9, affinity purified	Recognizes 60-65 kDa band corresponding to Sox9 on Western blot of fetal mouse brain lysate	Bowman's gland and duct cells
Rat α–E-cadherin	Sigma U 3254	Rat embryonal carcinoma line PCC4 AZA R1 was used as immunogen. The antibody is a monoclonal IgG1 provided in rat ascites fluid from the DECMA-1 hybridoma line. Monoclonal Anti-E-Cadherin was selected against the mouse E-Cadherin.	It blocks both the aggregation of mouse embryonal carcinoma cells and the compaction of pre-implantation embryos. The antibody disrupts confluent monolayers of MDCK epithelial cells. (Sigma Datasheet)	Sustentacular cells (weakly) and Bowman's gland and duct cells (strongly)
Goat α–CD54	R&D systems, AF583	Recombinant extracellular domain from rat, affinity-purified (Accession Q00238, Gln 28 - Thr 493)	Blocks adhesion to ICAM-1, WB confirmed	HBCs
Rabbit α–PGP9.5	Cedarlane/Ultraclone RA95101	Human PGP9.5 protein purified from pathogen free human brain	Cross reacts with all mammalian species tested. {Wilson, 1988 #938}	Immature and mature OSNs
Rabbit α–CK 18	Abcam 52948	A synthetic peptide corresponding to residues on the C-terminus of human Cytokeratin 18	Detects a band of approximately 48 kDa on WB. (Abcam datasheet)	Sustentacular cells, Bowman's gland and duct cells
Mouse α–CK14	Vector #VP-C410	Synthetic peptide corresponding to C-terminus region of human keratin 14 (GKVVSTHEQVLRTKN) conjugated to thryoglobulin.	Selectively labels basal cells in skin, with a cytoplasmic distribution (Vector Labs Datasheet)	HBCs
Rabbit α–CK14	LabVision #RB-9020-P1	A synthetic peptide of 15 amino acid residues from the C-terminus of human keratin 14.	Identical staining as above Mouse α–CK14. Stains A431 cells and skin or squamous cell	HBCs

Primary antibody	Source and catalog number	Immunogen and preparation	Specificity	Cell Types Stained
			carcinoma (Lab vision data sheet)	
Mouse α–Ki67	BD-Biosciences, 556003 (clone B56)	22 aa Ki-67 repeat motif (APKEKAQPLEDLASFQELSQ)	Reacts with 345/395 kDa doublet on WB corresponding to Ki-67 Ag; B56 binding to cells blocked by clone MIB 1, the canonical α–Ki67 antibody	Proliferating cells
Rat α–NCAM	Abcam ab19782 (H28-123)	Glycoprotein fraction from neonatal mouse brain	Recognizes at the neural cell surface a triplet of glycoproteins neural BSP2, which is identical to NCAM (Abcam datasheet)	Immature and mature OSNs
Mouse α–neuron specific tubulin	Covance MMS-435P (TuJl)	Microtubules derived from rat brain.	Highly reactive to neuron specific Class III ß-tubulin (ßIII). Does not identify ß-tubulin found in glial cells.	Immature OSNs
Rabbit α–PCNA	Abcam ab2426-1	Synthetic peptide: DMGHLKYYLAPKIEDEEGS, corresponding to C terminal amino acids 243-261 of Human PCNA.	Detects a band of approximately 29 kDa (predicted molecular weight: 29 kDa) which can be blocked with PCNA peptide (ab2427) (Abcam datasheet)	Proliferating cells
α–vimentin	Santa Cruz, sc-7557	A synthetic peptide at the C-terminus of human vimentin	Detects a band of approximately 57 kDa which can be blocked with sc-7557 P (Santa Cruz datasheet)	LPi_{mm} cells
α–Thy1.2	eBioscience, 14-0902 (clone 53-2.1)	Mouse thymus/spleen	Reacts with mouse CD90.2 (also known as Thy1.2, a GPI-linked membrane molecule; eBioscience datasheet)	LP-derived fibroblasts
α–PECAM	BD Bioscience, 550274 (clone MEC13.3)	129/Sv mouse-derived endothelioma cell line tEnd.1	Stains endothelial cells blood vessels in spleen, lung, heart and thymus (BD-Bioscience data sheet)	LP-derived endothelial cells